BUTTERWORTH HEINEMANN

Polymer Vol. 36 No. 24, pp. 4621–4637, 1995

0032-3861/95/$10.00 + 0.00

Impact-modified nylon 6/polypropylene blends: 3. Deformation mechanisms

A. González-Montiel, H. Keskkula and D. R. Paul*
Department of Chemical Engineering and Centre for Polymer Research, The University of Texas at Austin, Austin, TX 78712, USA
(Received 21 December 1994; revised 4 April 1995)

The processes that occur during the deformation of nylon 6/polypropylene blends modified with maleated rubbers were identified by dilatometric measurements and electron microscopy. These toughening mechanisms were found to depend on the type of rubber used as modifier (ethylene–propylene random copolymer, EPR-*g*-maleic anhydride (MA), or styrene–ethylene/butylene–styrene triblock copolymer, SEBS-*g*-MA), and on the relative ratio of nylon 6 to polypropylene (PP) in the blend. Blends based on EPR-*g*-MA showed significant volume dilation during deformation in a low strain rate tensile test. Electron microscopy techniques revealed that the main dilational mechanism in these blends is cavitation of the rubber dispersed as particles in the nylon 6 phase and at the nylon 6/PP interface. Similar results were obtained for specimens deformed in a high speed impact test. Except for one composition, nylon 6/PP blends modified with SEBS-*g*-MA showed negligible changes in volume during slow tensile deformation, and no indication of dilational processes (as determined by electron microscopy) was found in broken specimens deformed under notched Izod impact conditions. However, cavitation of the rubber particles was observed in 80/20 nylon 6/SEBS-*g*-MA blends deformed in the high speed impact test. This indicates that under appropriate stress and strain conditions, cavitation of SEBS-*g*-MA particles can occur. The structure and properties of the rubber and its particle size are factors that contribute to the differences in the extent of cavitation of nylon 6/PP blends modified with SEBS-*g*-MA or EPR-*g*-MA.

(Keywords: nylon 6; polypropylene; blends)

INTRODUCTION

Blends of nylon 6 and polypropylene (PP) can be effectively toughened (and compatibilized) using maleated rubbers such as ethylene–propylene random copolymers, EPR-*g*-maleic anhydride (MA), and styrene–ethylene/butylene–styrene triblock copolymers (SEBS-*g*-MA)[1–8]. The two rubbers produce blends with equivalent toughness at room temperature[8]. The basis for compatibilization of nylon 6/PP blends by these rubbers is relatively well understood; however, many of the details of how they produce toughness in these blends are not known.

Deformation mechanisms of rubber-toughened polymers have received considerable attention during the last two decades[9–34]; however, an understanding of the role of the rubber particles in the deformation process is still evolving. Recent studies indicate that cavitation of the rubber particles is necessary to relieve the triaxial tension ahead of the crack tip and allow the matrix to shear yield, thus absorbing energy and stopping crack propagation[11,19,20,23,26,33,35,36]. There is abundant literature on the modes of deformation of toughened polyamides[10,11,13,14,20,22,26,31,34,37–43]; however, there are still points of disagreement. Some reports claim cavitation of the rubber and shear yielding of the matrix as the main mechanisms[11,19,26,28,31,33,37,38,44], while others maintain that crazing, fibrillation of the matrix and crack blunting are also possible[25,37,38,45–47]. The deformation mechanism of impact polypropylenes is reported to depend very sensitively on strain rate and temperature. High temperatures and low strain rates favour shear yielding, whereas low temperatures and high strain rates favour crazing[27,48–51]. Studies on the deformation mechanisms of nylon 6/PP blends or toughened versions of these materials have not been reported to date.

This paper explores the processes that occur during deformation of rubber-modified nylon 6/PP blends using tensile dilatometry and electron microscopy. Tensile dilatometry involves measurement of volume strain during the slow uniaxial deformation of a polymer sample and has proven useful to elucidate the various processes that occur during tensile testing of single-phase and multiphase systems[10,12,15,16,18,29,50,52,53]. It is possible to estimate the contribution of shear yielding versus dilational processes (crazing, cavitation, voiding, etc.) to the post-yield deformation of the specimen. Deformation by shear yielding occurs essentially without change of volume, and the total volume strain beyond the yield point is roughly that associated with the deformation in the elastic zone (i.e. Poisson dilation). Deformation by dilational processes such as crazing, voiding and cavitation occurs with a significant increase of volume strain. Tensile dilatometry cannot distinguish between these different processes, so it is useful to complement such

* To whom correspondence should be addressed

measurements with electron microscopy techniques. Because strain rate can have a strong effect on the type of deformation that occurs (as noted earlier), especially in polypropylene[27,48–50], the toughened nylon 6/PP blends of interest here were examined using both a low speed tensile test and a high speed impact test. All the blends studied here show tough behaviour at room temperature, as reported elsewhere[8]; however, different levels of toughness, as measured in an Izod impact test, are obtained by varying the nylon 6/PP ratio of the blend, as summarized in *Figure 1*.

EXPERIMENTAL

Materials

The nylon 6 used here (Capron 8207F) was a commercial material from Allied Signal with $\overline{M}_n = 22\,000$. The polypropylene was a homopolymer from Huntsman (PP 5520) with a melt flow rate (*MFR*) of 5.0 and $\overline{M}_w = 347\,000$. *Table 1* shows some pertinent information about the rubber modifiers used in this work. A blend of unfunctionalized SEBS and SEBS-*g*-MA rubbers was used to achieve the same maleic anhydride content of the EPR-*g*-MA rubber (1.14% MA). Details on the preparation and use of such mixtures can be found elsewhere[8,54].

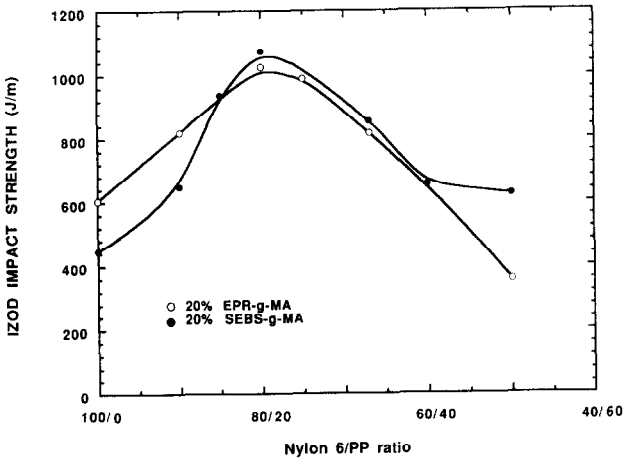

Figure 1 Room temperature Izod impact strength of nylon 6/polypropylene blends modified with 20% (based on the total mass of the ternary blend) EPR-*g*-MA or SEBS-*g*-MA as a function of the ratio of nylon 6 to polypropylene in the blend[8]

Blend preparation

All the materials were predried before melt processing. Nylon 6 was dried in a vacuum oven for a period of 16 h at 80°C, while the rubber and polypropylene were dried in a convection oven also for 16 h at 80°C. The blends were prepared in a Killion single-screw extruder ($L/D = 30$, $D = 2.54$ cm) operating at 240°C and 40 rev min^{-1}. The extruded materials were injection moulded into tensile and impact specimens (3 mm thickness) using an Arburg Allrounder injection-moulding machine. All specimens were kept in a desiccator under vacuum until they were tested. Tensile specimens were used for the tensile dilatometry test, while impact specimens were used for the single-notch three-point bend (SN3PB) test.

Tensile dilatometry

Volume strain during tensile deformation was measured using a liquid displacement dilatometer similar in design to that of Coumans and Heikens[12,52,55]. Pertinent details on the operation of and treatment of data obtained with this dilatometer have been previously reported by Schwarz *et al.*[16]. Tensile deformation of the specimen was conducted in a water-filled chamber attached to an Instron tensile tester. The change in volume of the sample due to deformation was monitored by the water level in a capillary connected to the chamber and detected by a differential pressure transducer. This signal and that from the Instron load cell were recorded simultaneously. Global longitudinal strain (ε) was followed by the rate of crosshead travel, which was always at 0.5 cm min^{-1}. While pure nylon 6 and PP showed clear macroscopic evidence of necking, most of the alloys did not.

The mechanical properties of polyamides such as nylon 6 are strongly affected by water. The water acts as a plasticizer, reducing both yield stress and modulus. Water sorption also affects the deformation mechanisms of neat and impact-modified polyamides[33,47,56,57]. Samples to be used in the liquid displacement dilatometer were stored in a desiccator and tested within 15 min of contact with the water in the dilatometer chamber. Control experiments showed that this brief exposure to water had no measurable effect on the observed yield stress and modulus of the blends and produced a negligible contribution to the observed volume change during the deformation experiment. The latter was demonstrated by two types of experiments. Samples containing nylon 6 showed negligible

Table 1 Rubber modifiers

Designation used here	Material (commercial designation)	Composition by weight	Molecular weight	Density (g cm^{-3})	Source
SEBS	Styrene–ethylene/butylene–styrene (Kraton G 1652)	29% styrene	Styrene block = 7000 Ethylene–butylene block = 37 500	0.91	Shell
SEBS-*g*-MA	(Styrene–ethylene/butylene–styrene)-*g*-maleic anhydride (Kraton G 1901 X)	29% styrene 1.84% MA	Not available	0.91	Shell
EPR-*g*-MA	Ethylene–propylene rubber grafted with maleic anhydride (Exxelor 1803)	43% ethylene 57% propylene 1.14% MA	Not available	0.85	Exxon

volume change in a static test (no crosshead movement) during a time period equal to the typical dilatometer experiment. A pure nylon 6 sample showed essentially no volume change in the post-yield region, as expected for a material that shear yields.

Microscopy

Scanning and transmission electron microscopy (SEM, TEM) were used to complement the data obtained by dilatometry. Samples excised from specimens after the slow speed uniaxial deformation of the dilatometry test and after a high speed deformation impact test were used for this purpose. A block, approximately $7 \times 12 \times 3$ mm, was cut from the whitened zone of each tensile dilatometry specimen (*Figure 2a*) and then cryo-fractured to expose the inner deformed morphology (*Figure 2b*). The block was first notched (100 μm radius) in the longitudinal direction using a circular saw, after which a sharp notch of approximately 1–2 mm was made using a fresh razor blade. The block was submerged in liquid nitrogen for a period of 10 min and then quickly retrieved and fractured by tapping a wedge into the coarse notch. The resulting surfaces were on a plane parallel to the applied stress and showed the microstructure of the deformed specimen. Cryo-fractured surfaces of samples that had not been previously strained were shown to be featureless by SEM, indicating that this preparation technique does not introduce artefacts.

An instrumented drop-dart impact tester (Dynatup 8200) was used to deform specimens in an SN3PB set-up (see *Figure 3a*). The velocity of impact was 3.4 m s^{-1}. An arrested or incomplete fracture was generated by adjusting the stops on the drop tower so that the falling weight or tup stopped before the crack completely penetrated the specimen. In this way the fracture stopped at approximately half the width of the specimen. After impact testing, the deformed region of the specimen was cryo-fractured following a procedure similar to the one used for the tensile dilatometry specimens (*Figure 3b*). A block containing the damaged zone was first notched with a circular saw and then with a fresh razor blade. This procedure was repeated on both sides of the block to allow a clean fracture to propagate through the deformed zone ahead of the crack tip. The sample was cooled in liquid nitrogen for 10 min and then quickly fractured by tapping a sharp wedge into one of the notches. The half containing the subfracture surface was selected for SEM and TEM observation. The exposed surface of this half was a plane perpendicular to the propagating crack and ahead of the shear-yielding zone, which enabled observation of features such as crazing, cavitation of rubber, etc. before they were affected by the yielding of the specimen.

Samples for SEM were first sputtered with a layer of gold–palladium and then observed in a JEOL 35C scanning electron microscope operating at 25 kV. Samples for TEM were stained for a period of 12 h using ruthenium tetroxide (RuO_4) vapours in the case of SEBS-*g*-MA-based blends or a 0.5% aqueous RuO_4 solution in the case of EPR-*g*-MA-based blends. After staining, the samples were sectioned at −25°C using a Reichert–Jung Ultracut E microtome. The thin sections (20–50 nm) were viewed in a JEOL 200CX transmission electron microscope operating at 120 kV.

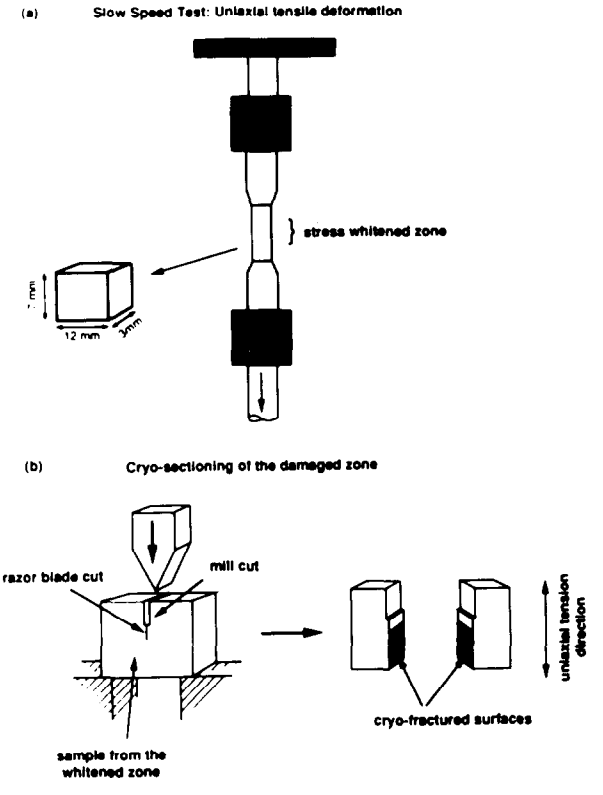

Figure 2 Schematics of a uniaxially strained test bar showing (a) the location and size of the sample excised from the specimen and (b) the cryo-sectioning technique used to expose damaged zones in a plane parallel to the deformation direction

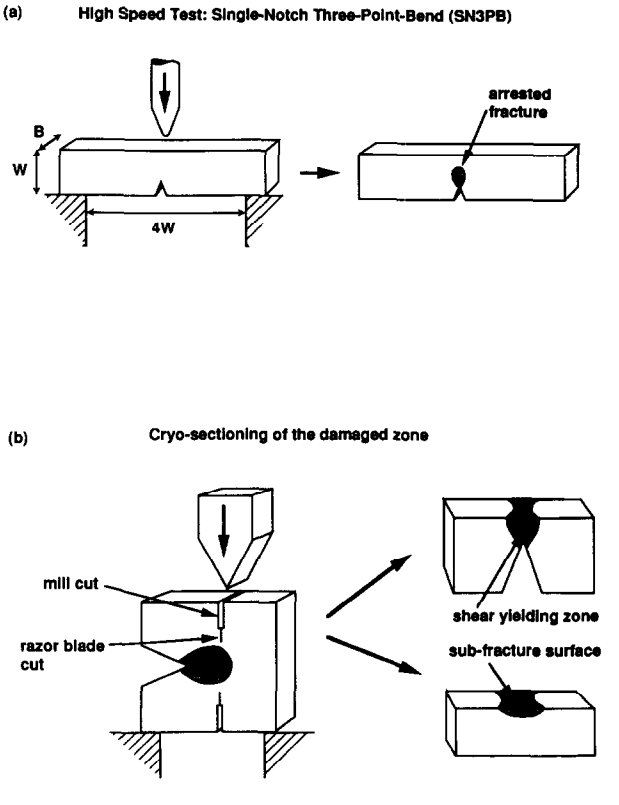

Figure 3 Schematics of (a) a single-notch three-point bend (SN3PB) specimen before and after failure (specimen dimensions $B = 3.0$ mm, $W = 12.6$ mm) and (b) the cryo-sectioning procedure used to expose the damaged region ahead of the arrested fracture

DEFORMATION MECHANISMS AT LOW STRAIN RATE: UNIAXIAL TENSILE DEFORMATION

Blends modified with EPR-g-MA rubber

Figure 4 shows plots of stress–strain and volume strain–strain for 80/20 blends of nylon 6/EPR-*g*-MA and polypropylene/EPR-*g*-MA. These represent the composition extremes for rubber-modified nylon 6/PP blends. A significant increase in volume strain is observed during the deformation of the 80/20 nylon 6/EPR-*g*-MA blend (*Figure 4a*). The initial change in volume before yielding is related to the elastic or recoverable volume strain, while the post-yield volume change is the result of a non-recoverable volume dilation mechanism such as crazing, rubber cavitation, voiding or debonding. Since the slope of the volume strain–strain plot in the post-yield region is less than 1, some shear yielding evidently occurs in addition to whatever volume dilation process is occurring. *Figure 4b* shows a similar plot for the 80/20 PP/EPR-*g*-MA blend. Again, an initial volume increase due to the Poisson ratio effect is noted; however, only a very small post-yield change in volume is observed, indicating that the deformation is primarily by shear yielding. Information in the literature for similar blends is in good agreement with the above results[10,27,33,34,48].

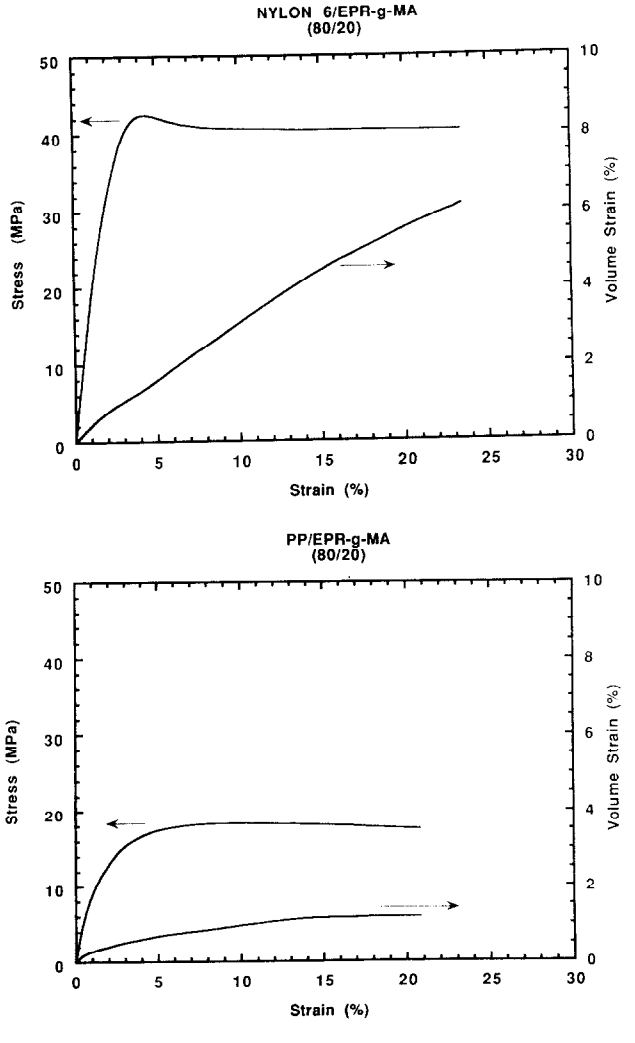

Figure 4 Stress–strain and volume strain–strain curves for (a) nylon 6 and (b) polypropylene modified with 20% EPR-*g*-MA

Figure 5a shows volume strain–strain curves for nylon 6/PP blends modified with 20% EPR-*g*-MA. An increase in volume strain in the post-yield region is noted for all these blends. The slope of the volume strain–strain plot changes with both the nylon 6/PP ratio and the longitudinal strain, indicating that the contribution of

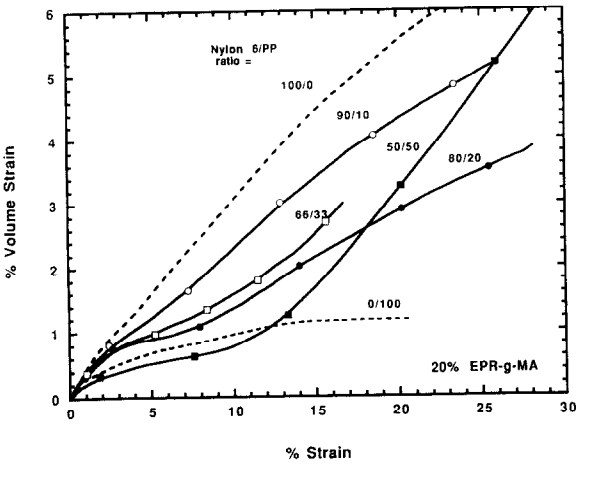

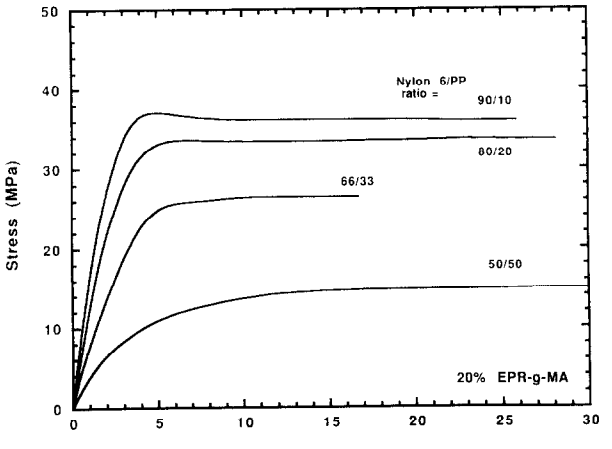

Figure 5 (a) Volume strain–strain curves and (b) stress–strain curves for nylon 6/PP blends modified with 20% EPR-*g*-MA

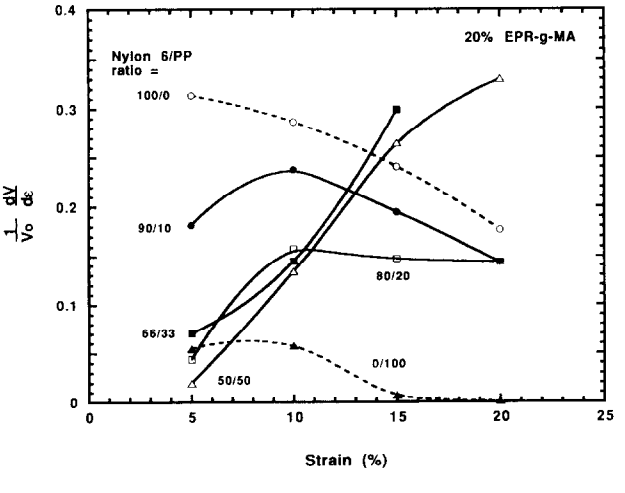

Figure 6 Slope of the volume dilation–strain curves versus longitudinal strain for nylon 6/PP blends modified with 20% EPR-*g*-MA

dilational processes to the volume strain changes with these two variables. Also, the onset of the dilational processes occurs at higher longitudinal strains with increasing PP content in the blend. This last observation relates to the stress–strain behaviour of the blends (see *Figure 5b*). Blends with low polypropylene contents (90/10 and 80/20 nylon 6/PP ratios) yield at lower longitudinal strains than blends with higher PP contents (66/33 and 50/50 nylon 6/PP ratios). This change in the yielding behaviour shifts the beginning of the non-elastic increase in volume strain towards higher longitudinal strains.

The slopes of the volume dilation curves are shown in *Figure 6* as a function of elongational strain. Binary blends of nylon 6 with EPR-*g*-MA and polypropylene with EPR-*g*-MA show significant decreases in slope as the uniaxial strain increases from 5 to 20%, suggesting that dilational processes are more prevalent at the beginning than during the later stages of the deformation. Ternary blends with relatively low polypropylene contents (90/10 and 80/20 nylon 6/PP ratios) first show an increase in slope going from 5 to 10% strain and then a decrease in slope with further increases in strain. The initial increase in slope is probably related to the high yield elongation of these materials. In contrast, for blends with 66/33 and 50/50 nylon 6/PP ratios, the slope always increases with strain. This indicates that the dilational mechanisms become more prominent in the later stages of the deformation. In all the above, the highest value for the slope (in the 5–20% strain range) is 0.32; thus, in addition to whatever dilational process is occurring, the matrix also undergoes extensive shear yielding.

The observed changes in volume strain seem to be related to the morphology these blends have prior to deformation, which has been described in detail elsewhere[8,54]. For blends which have a nylon 6/PP ratio of 90/10 or 80/20, the rubber and the polypropylene are dispersed in a matrix of nylon 6. The rubber also forms a relatively thick, non-uniform layer between the nylon 6 phase and the polypropylene domains. The blend with the 66/33 nylon 6/PP ratio has a co-continuous morphology where rubber particles are located in the nylon 6 and polypropylene phases and at the nylon 6/PP interface. Polypropylene particles are dispersed in the nylon 6 phase and vice versa. In the blend with a 50/50 nylon 6/PP ratio, both nylon 6 and rubber are dispersed in a continuous matrix of PP, and the rubber is found both in the nylon 6 phase and at the nylon 6/PP interface. Blends where nylon 6 is the continuous phase show a decrease in the post-yield volume strain–strain slope with both the PP content and the longitudinal strain, while in the blend with a co-continuous morphology and the blend where the PP is the matrix phase (66/33 and 50/50 nylon 6/PP ratios, respectively) the slope increases with increasing longitudinal strain.

SEM photomicrographs of deformed samples from the dilatometric test are shown in *Figure 7*. The observed surface was generated by the cryo-sectioning procedure explained earlier (see *Figure 2b*), and is from a plane parallel to the tensile axis. The photomicrograph of a deformed 80/20 nylon 6/EPR-*g*-MA specimen suggests that cavitation of the rubber particles dispersed in the nylon 6 has occurred, and TEM results described later confirm this. It is reasonable to assume that this process is connected to the post-yield dilation observed. The cavities seem to line up in bands at a certain angle with respect to the direction of the applied stress; such oriented bands of cavitated particles have been reported before[11,26,33], and are associated with planes of shear yielding within the nylon 6 matrix. Rubber cavitation is believed to precede and induce shear yielding of the matrix. That dilation continues throughout the deformation process could be related to continued growth of the already-formed cavities or growth of this deformation zone within the tensile specimen as the global strain increases. SEM photomicrographs are shown in *Figures 7b–e* for the rubber-modified nylon 6/PP blends. Blends where the polypropylene is the dispersed phase (90/10 and 80/20 nylon 6/PP ratios) appear to develop holes in the region of the interface between the PP particles and the nylon 6 matrix. This does not necessarily mean debonding between nylon 6 and polypropylene, since previous morphological observations have suggested that there is a layer of maleated rubber between these components. TEM evidence shown later suggests that the hole formation may be a result of the cavitation of this rubber layer. In any case, this is another source of volume dilation for these blends in addition to any cavitation of the rubber particles in the nylon 6 matrix that may occur. It is also apparent that as the nylon 6/PP ratio decreases from 90/10 to 80/20, cavitation of the rubber particles in the nylon 6 decreases and more voiding at the interface is observed. The blend with the co-continuous morphology (66/33 nylon 6/PP ratio) also shows signs of cavitation; however, precise location of the cavitation is difficult since the co-continuous morphology of this blend cannot be discerned by SEM. *Figure 7e* shows that fine holes are also present in the blend where PP is the matrix (50/50 nylon 6/PP ratio). In this case, holes seem to form around the nylon 6 particles, and some filaments can be seen bridging the space between the particles and the PP phase.

There is a good correlation between the stress dilatometry results and the SEM photomicrographs of the deformed specimens. Cavitation of the rubber particles in the nylon 6 matrix and void formation in the region of the nylon 6/PP interface are the mechanisms that generate the increase in volume strain observed during tensile deformation. The decrease in volume dilation with increasing PP content (for blends where the PP and rubber are dispersed in a nylon 6 matrix) seems to be related to the frequency of hole formation at the interface between nylon 6 and PP. Voiding at the interface probably occurs at a lower stress than that necessary to cavitate the rubber particles dispersed in the nylon 6 matrix; therefore, when more PP particles are present, fewer rubber particles dispersed in the nylon 6 can cavitate and the volume strain is reduced. The increase in volume strain for the blend with a co-continuous morphology (66/33 nylon 6/PP ratio) is also due to cavitation of the rubber, although in this case voiding at the interface is not as extreme as in the blends that have a nylon 6 matrix. This may indeed be the reason for the change of behaviour observed in the slope of the volume strain–strain curve. For blends where PP is the continuous phase, the increase of the post-yield volume strain slope could be attributed to the formation of voids or holes at the interface of the nylon 6 particles (see *Figure 7e*), and also to additional dilational

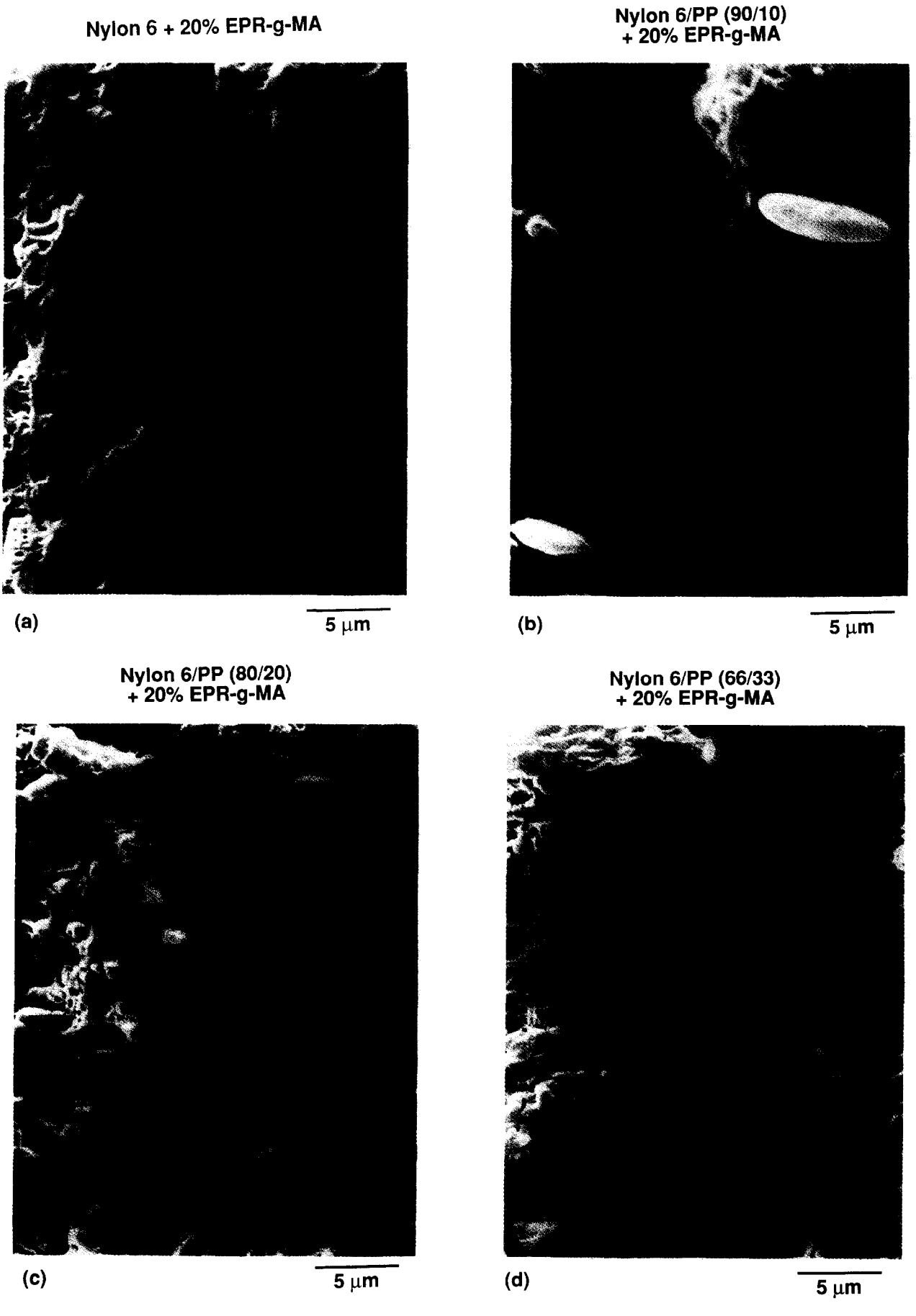

Figure 7 SEM photomicrographs of cryo-fractured surfaces of nylon 6/PP blends modified with 20% EPR-*g*-MA and deformed in uniaxial tension for the nylon 6/PP ratios (a) 100/0, (b) 90/10, (c) 80/20 and (d) 66/33

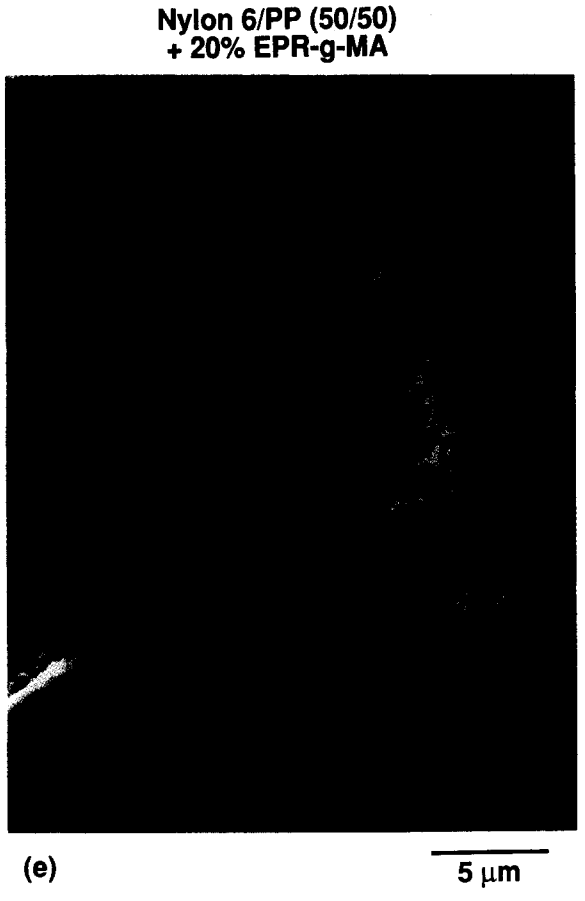

Figure 7e SEM photomicrograph of cryo-fractured surfaces of nylon 6/PP blends modified with 20% EPR-*g*-MA and deformed in uniaxial tension for the nylon 6/PP ratio 50/50

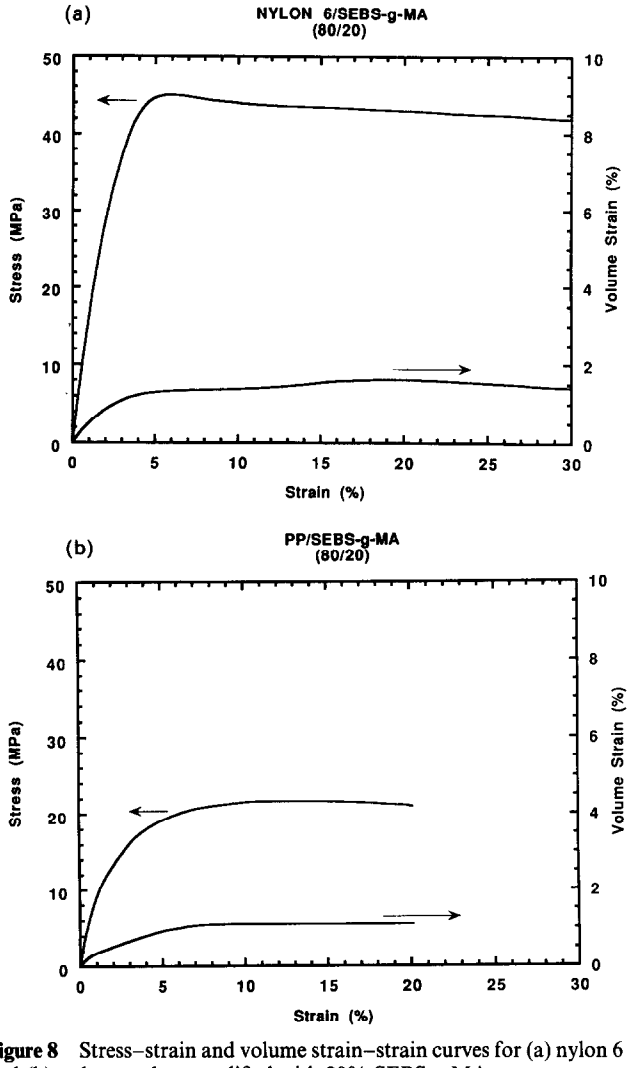

Figure 8 Stress–strain and volume strain–strain curves for (a) nylon 6 and (b) polypropylene modified with 20% SEBS-*g*-MA

mechanisms such as crazing. Jang[49] has shown that the deformation mechanism in rubber-modified polypropylene depend on the size of the rubber particles, viz. rubber particles with diameters larger than 0.5 μm are able to nucleate crazes. Thus, the nylon 6 and rubber particles dispersed in the polypropylene can potentially nucleate crazes in the PP phase. This could explain the accelerated increase in the slope of the volume strain–strain curves at high elongational strain.

Blends modified with SEBS-g-MA rubber

The volume strain plots in *Figures 8a* and *8b* for 80/20 nylon 6/SEBS-*g*-MA and 80/20 PP/SEBS-*g*-MA blends show negligible volume change with deformation in the post-yield region for these blends. Obviously the matrix in both cases deforms by shear yielding. The results for nylon 6 blends with SEBS-*g*-MA are in strong contrast with those in *Figure 4a* for similar blends containing EPR-*g*-MA. It seems that SEBS-*g*-MA particles are not able to cavitate in uniaxial tension at low strain rates, whereas EPR-*g*-MA particles readily cavitate under these conditions. The PP blend with SEBS-*g*-MA (*Figure 8b*) shows behaviour similar to that for the blend modified with EPR-*g*-MA; no important dilational mechanisms occur at this low strain rate, as reported by other authors[27,48–50].

Figure 9a shows volume strain plots for blends of nylon 6 and PP modified with 20% SEBS-*g*-MA rubber. All but one of the blends deform without change in volume strain in the post-yield region. The blend with a 66/33 nylon 6/PP ratio shows a small increase in volume at high deformations. The volume dilation in this case is smaller than that of the equivalent blend modified with EPR-*g*-MA. *Figure 9b* shows the corresponding stress–strain curves for these blends. The yield stress decreases with increasing PP content, as in the case of EPR-*g*-MA-based blends.

SEM photomicrographs of the cryo-fractured surfaces from deformed specimens are shown in *Figure 10*. No hole formation is apparent in this series of blends regardless of the PP content. The fracture surface seems to become more rough as the PP content of the blend is increased, but still no hole formation is observed. It is important to note that the photomicrograph of the 66/33 nylon 6/PP blend does not show any signs of volume change stemming from rubber cavitation, debonding or crazing; however, tensile dilatometry does show that some increase in volume strain occurs during the post-yield deformation of this blend. This discrepancy might be attributed to the occurrence of a dilational process that cannot be discerned by SEM. The morphology of this blend has been described in a previous publication[8] as one of finely interlocked co-continuous nylon 6 and polypropylene phases where the SEBS-*g*-MA rubber locates in the nylon 6 phase and at the interface between nylon 6 and PP. The observed increase in volume strain could be attributed to the

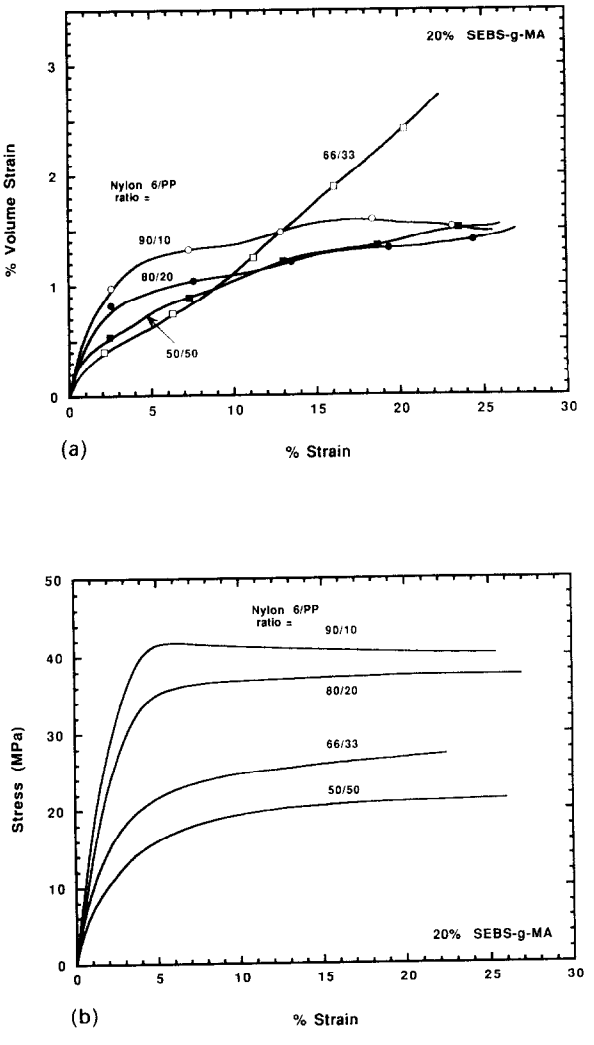

Figure 9 (a) Volume strain–strain curves and (b) stress–strain curves for nylon 6/PP blends modified with 20% SEBS-*g*-MA

cavitation of the rubber located at the interface between nylon 6 and PP and in the nylon 6 phase. The interfacial cavities might either be too small to be detected by SEM or tend to close after the tensile sample is relieved from the imposed stress. TEM evidence shown later in this paper confirms that the cavitation of the SEBS-*g*-MA rubber particles dispersed in nylon 6 is possible under appropriate stress and strain conditions.

The results in *Figures 4–10* illustrate that the extent of post-yield volume dilation of rubber-modified nylon 6/PP blends strongly depends on the type of rubber used. Under these conditions, the EPR-*g*-MA rubber particles readily cavitate in these blends, whereas SEBS-*g*-MA particles seem to do it only in one case (66/33 nylon 6/PP blend). The mechanical properties of the elastomer evidently affect its ability to cavitate under stress[11,26,37,38,43]. EPR-*g*-MA and SEBS-*g*-MA rubbers differ in their structures, glass transition temperatures and moduli; the former is a single-phase random copolymer of ethylene and propylene with a T_g of −45°C, while the latter is a microphase-separated triblock copolymer whose olefinic midblock has a T_g of −38°C. The polystyrene microdomains act as physical crosslinks and as a filler or reinforcement. These hard domains are in part responsible for the higher modulus of SEBS-*g*-MA compared to that of the EPR-*g*-MA rubber. The differences in deformation response observed here for nylon 6/PP blends are no doubt related to these issues.

DEFORMATION AT HIGH STRAIN RATES: SINGLE-NOTCH THREE-POINT BEND (SN3PB)

Blends modified with EPR-g-MA

Figure 11 shows a series of SEM photomicrographs of specimens prepared by the cryo-sectioning procedure (*Figure 3b*) following deformation by the high speed SN3PB technique described earlier. The compositions of the blends in *Figure 11* match those in *Figure 7*. Cavitation of the rubber particles is seen in the 80/20 nylon 6/EPR-*g*-MA blend (*Figure 11a*), similar to what was observed at low speeds during tensile dilatometry. The roughness of the exposed surface is attributed to the sponge-like structure of the cavitated region which makes it very difficult to obtain a flat surface using cryo-sectioning. Hole formation is also observed in rubber-modified nylon 6/PP blends. Blends where the PP is the dispersed phase (90/10 and 80/20 nylon 6/PP ratios) show cavitation of the rubber particles dispersed in the nylon 6 and voiding at the interface between the nylon 6 and the dispersed PP particles. In some cases, filaments connect the PP particles to the nylon 6 matrix (see the arrows in *Figures 11b* and *11c*). The sample with a co-continuous morphology (66/33 ratio) also shows cavitation; as in *Figure 7d*, it is very difficult to determine whether hole formation at the nylon 6/PP interface also occurs or not. The photomicrographs in *Figure 11* show essentially the same features observed for the specimens of *Figure 7* that were deformed in the low speed tensile dilatometer test.

Transmission electron microscopy techniques were used to explore more exactly the location of the holes formed in the deformed regions. *Figure 12* shows photomicrographs of a deformed 80/20 blend of nylon 6 and EPR-*g*-MA rubber. *Figure 12a* shows a bright field photomicrograph of this blend where the polyamide phase is stained with RuO_4. Holes within the rubber particles are apparent, although they are not readily distinguishable from the undeformed rubber particles. *Figure 12b* shows a dark field version of the photomicrograph in *Figure 12a*, so the holes in the sample appear dark and the rest of the sample bright. Comparing both figures, it is possible to confirm that holes form in the rubber particles during the deformation. These observations are in agreement with those from *Figures 7a* and *11a*.

Figure 13 shows photomicrographs of an 80/20 nylon 6/PP blend (modified with 20% EPR-*g*-MA) before (*Figure 13a*) and after (*Figure 13b*) deformation. The specimens were stained with an RuO_4 solution for 12 h. In this way, only the rubber at the interface between nylon 6 and PP is selectively stained (details of the staining technique have been described in a previous paper[8]). The grey particles are polypropylene, while the nylon 6 matrix with unstained rubber and PP dispersed in it appears as a grey background. The rubber forms a layer of non-uniform thickness around the polypropylene particles and some rubber particles seem to be near or within this layer. These features are important elements for understanding the morphology of the deformed sample (*Figure 13b*). The deformed sample

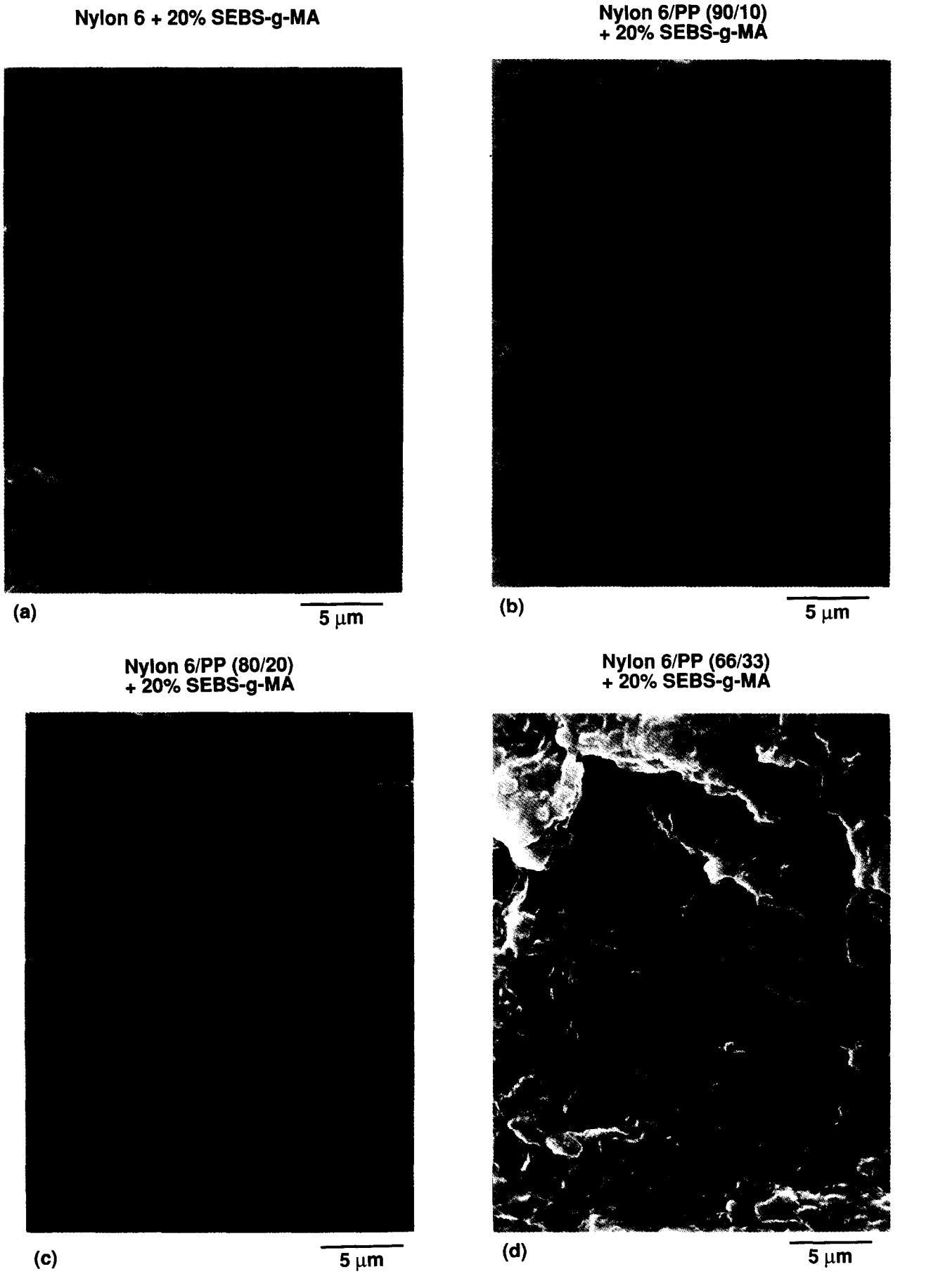

Figure 10 SEM photomicrographs of cryo-fractured surfaces of nylon 6/PP blends modified with 20% SEBS-*g*-MA and deformed in uniaxial tension for the nylon 6/PP ratios (a) 100/0, (b) 90/10, (c) 80/20 and (d) 66/33

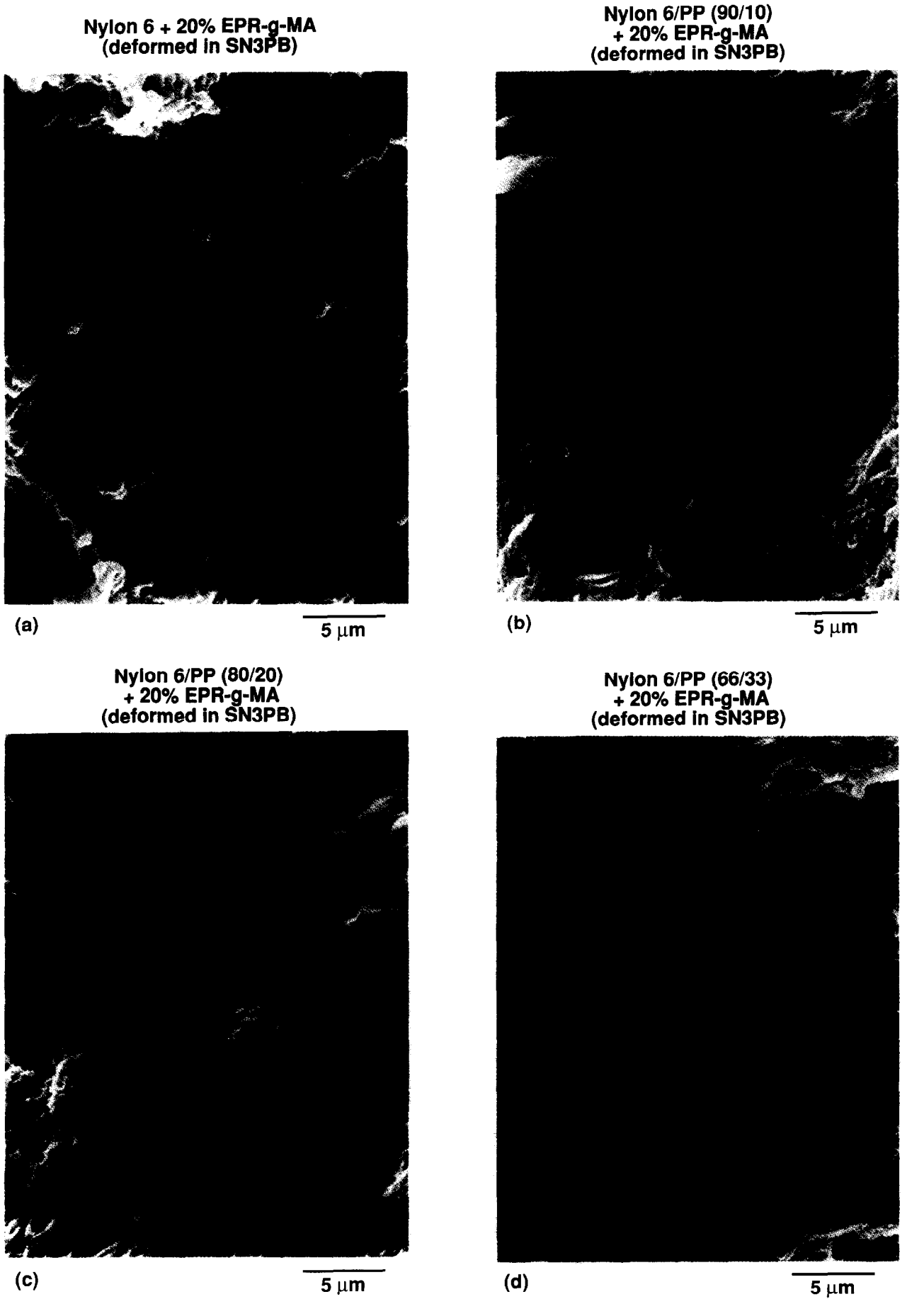

Figure 11 SEM photomicrographs of cryo-fractured surfaces of nylon 6/PP blends modified with 20% EPR-*g*-MA and deformed in the SN3PB impact test for the nylon 6/PP ratios (a) 100/0, (b) 90/10, (c) 80/20 and (d) 66/33

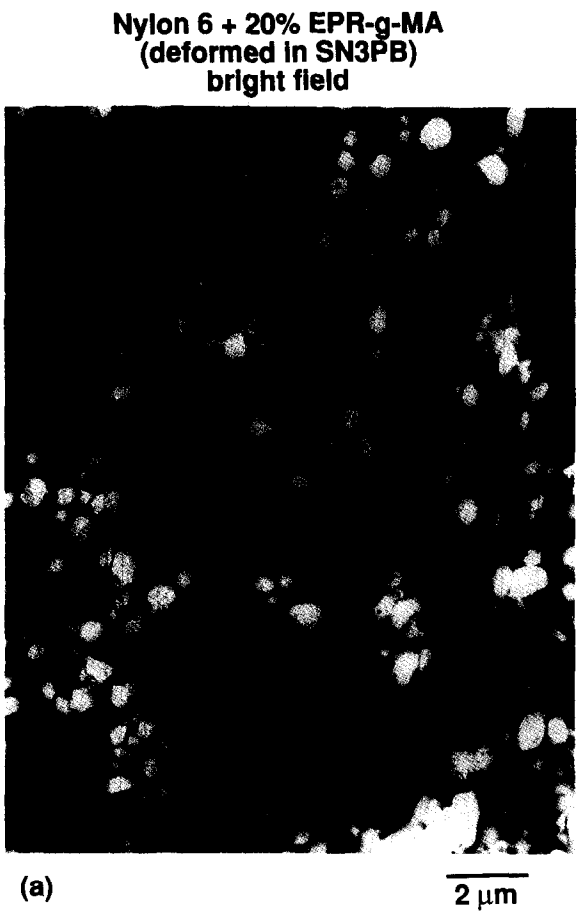

Figure 12 TEM photomicrographs of the deformed zone of rubber-toughened nylon 6 (20% EPR-*g*-MA) under (a) bright field and (b) dark field conditions. The blend is stained with RuO_4

Figure 13 TEM photomicrographs of an 80/20 nylon 6/PP blend (modified with 20% EPR-*g*-MA) (a) before deformation and (b) after the SN3PB test. The rubber is stained with a 0.5% aqueous solution of RuO_4

was stained similarly, so the dark zone around the dispersed particles is the EPR-*g*-MA rubber. Hole formation at the interface between nylon 6 and PP is evident. The holes appear to form at opposite extremes of the particles and grow from there. It is not possible to determine the direction of stress in these photographs, but most likely the holes form at the poles of the particles. Thin fibrils span the holes to interconnect the PP particles to the nylon 6 matrix. Comparing *Figures 13a* and *13b*, we conclude that the holes originate by the cavitation of the rubber particles and the rubber layer located between the nylon 6 and PP domains. The cavitation of the rubber in the interfacial layer seems to initiate in thick regions of this layer or at rubber particles embedded in this layer. It is not clear whether the rubber particles dispersed in the nylon 6 cavitate since these particles are unstained in this photomicrograph.

TEM photomicrographs of the 66/33 nylon 6/PP blend modified with 20% EPR-*g*-MA are shown in *Figure 14*. This blend showed hole formation during the SN3PB deformation (see *Figure 11d*); however, a clear assessment of where the holes occur was not possible owing to the limitations of the SEM technique. *Figure 14a* shows the undeformed morphology of the blend stained with RuO_4 as before. Again the rubber is the dark phase, while the polypropylene and nylon 6 appear as light phases. The nylon phase was intentionally understained so that the rubber particles and polypropylene particles dispersed in it would not be discernible. This photomicrograph clearly shows the EPR-*g*-MA rubber located in the PP phase and at the interface. The locations of rubber and PP in the nylon 6 phase can be seen in *Figure 14b*, where the nylon 6 is stained dark with phosphotungstic acid, while the rubber and polypropylene remain unstained. Rubber and polypropylene particles are dispersed in the dark nylon 6 phase; nylon 6 particles are also dispersed in the polypropylene phase. From these two photomicrographs it is apparent that the morphology of the blend is very complex: nylon 6 and polypropylene form co-continuous phases, but also form dispersed phases in each other. EPR-*g*-MA rubber seems to be located in both the nylon 6 and polypropylene phases and also at the interface between these two polymers. A photomicrograph of the same blend after the SN3PB test is shown in *Figure 14c*. The blend is stained in a similar way as in *Figure 14a*, but in this case the nylon 6 phase is stained by the RuO_4 (through longer exposure) and the rubber and PP particles dispersed in this phase are also visible. Holes in both the nylon 6 and PP phases are visible. The holes tend to locate at the interface between nylon 6 and polypropylene independent of whether these polymers form continuous or dispersed phases (see the arrows in *Figure 14c*). That is, holes form at the interface of the PP particles dispersed in the nylon 6 phase and also at the interface of nylon 6 particles dispersed in the polypropylene phase. These holes can be attributed to the cavitation of the rubber layer and rubber particles in the region of this layer.

The photomicrographs in *Figures 13* and *14* confirm that the volume dilation observed in nylon 6/PP blends modified with EPR-*g*-MA results from cavitation of the rubber particles dispersed in the nylon 6 and of the rubber at the interface with polypropylene. This conclusion is the same as that obtained from dilatometry and SEM observation of specimens subjected to slow tensile deformation. Shear deformation is not observed in these photomicrographs since the SEM and TEM specimens were excised from the subfracture region ahead of the shear yield zone. Therefore, only the initial step of the deformation mechanism (cavitation of the rubber) is observed.

Blends modified with SEBS-g-MA

Figure 15 shows SEM photomicrographs of cryo-fractured surfaces of blends modified with SEBs-*g*-MA. The exposed surface of a deformed 80/20 nylon 6/SEBS-*g*-MA blend (*Figure 15a*) does not show signs of rubber cavitation or other volume dilation mechanisms. The same is true for the nylon 6/PP blends (*Figures 15b–15d*). Surface roughness is apparent on some of the cryo-exposed surfaces, but no cavitation is observed. The damaged zone of the 66/33 nylon 6/PP blend shows a rumpled surface that resembles the shear-yielded regions observed by Speroni *et al.*[33] for the fracture of water-conditioned nylon 6. These photomicrographs appear to corroborate the stress dilatometry results described earlier for blends modified with this rubber.

TEM techniques were used to explore further these blends following deformation. *Figure 16a* shows the undeformed morphology of an 80/20 nylon 6/SEBS-*g*-MA blend stained with RuO_4. The polystyrene domains of the SEBS stain dark, so the rubber appears as dark-speckled particles in a grey background of nylon 6. Photomicrographs of nylon 6/SEBS-*g*-MA blends following deformation in the SN3PB test are shown in *Figures 16b* and *16c*. *Figure 16b* shows an unstained sample (equivalent to a dark field photomicrograph) where the observed small white particles are actually holes. *Figure 16c* is a high magnification photomicrograph of the same deformed sample stained with RuO_4. The holes observed in *Figure 16b* can now be confirmed to be cavitated SEBS-*g*-MA particles. The cavitation is not as widespread as observed for the nylon 6/EPR-*g*-MA blend, which probably explains why these holes were not detected in the SEM photomicrograph. It is important to note that even small rubber particles (below 0.2 μm) seem to be able to cavitate. In a previous section, it was noted that SEBS-*g*-MA rubber particles were not able to cavitate under the conditions used in the uniaxial tensile test; however, these particles appear to be able to cavitate under appropriate stress and strain rate conditions, i.e. triaxial stress and high strain rate conditions. An important point relevant to these observations is that a small whitened zone is observed ahead of the arrested fracture in the SN3PB specimens, whereas whitened zones are not observed when the fracture is complete as in an Izod impact test. This indicates that the procedure used to generate the arrested fracture is successful in preserving the cavitated particles before yield deformation of the matrix occurs with subsequent collapse of these holes.

TEM photomicrographs of an 80/20 nylon 6/PP blend modified with 20% SEBS-*g*-MA are shown in *Figure 17*. The morphology of the undeformed specimen, stained with RuO_4, is shown in *Figure 17a*. The rubber appears as a dark phase, nylon 6 stains grey and polypropylene remains unstained. The morphology is on the verge of co-continuity, but nylon 6 still forms the matrix with a tendency to break up into particles, whereas the polypropylene forms elongated domains. The rubber is

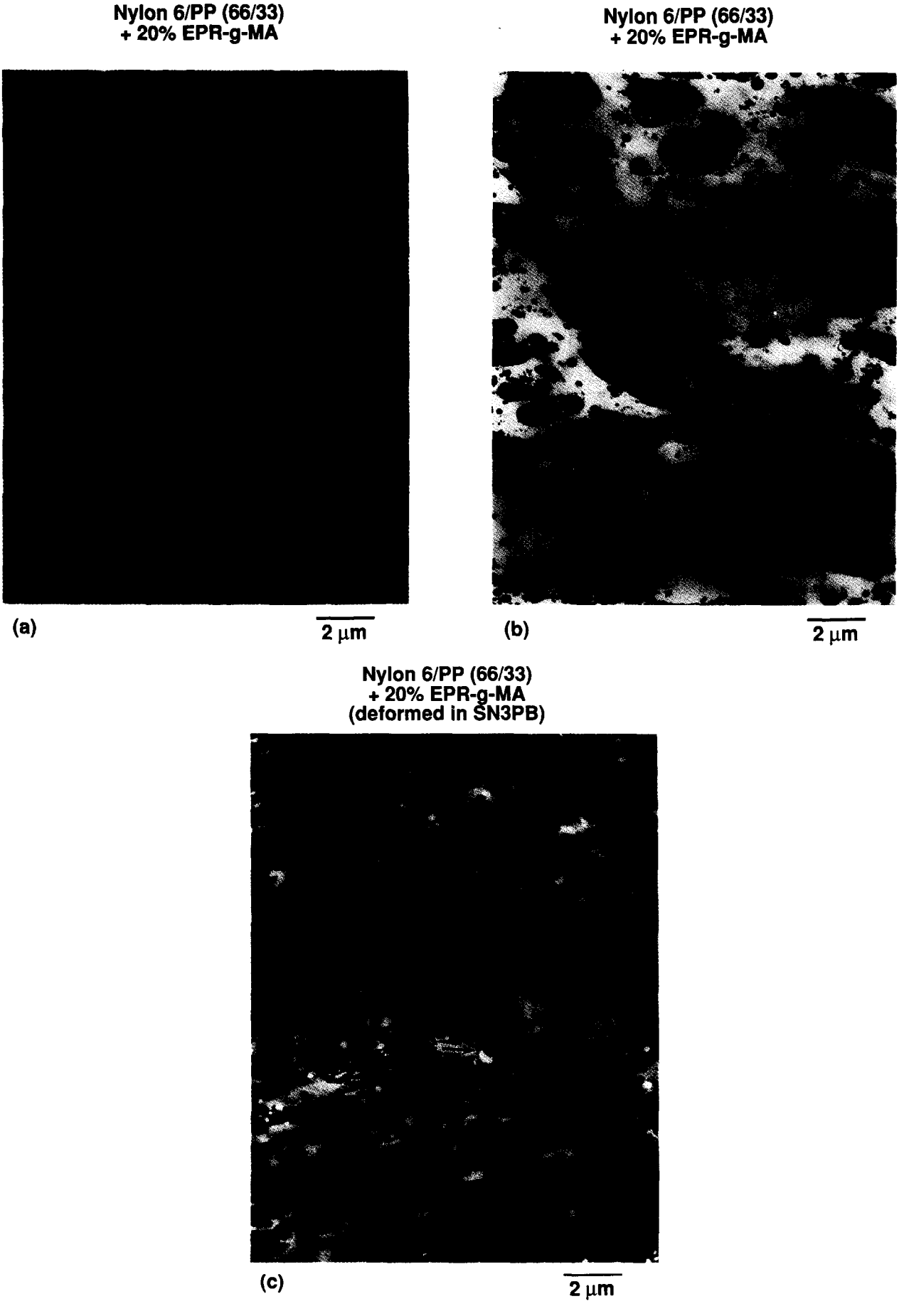

Figure 14 TEM photomicrographs of the 66/33 nylon 6/PP blend modified with 20% EPR-*g*-MA: undeformed sample stained with (a) a 0.5% aqueous solution of RuO_4 (the rubber at the nylon 6/PP interface and in the PP phase stains dark) and (b) phosphotungstic acid (polyamide phase stains dark). (c) Sample deformed in the SN3PB test and stained with a 0.5% aqueous solution of RuO_4. The arrows indicate the presence of holes in both the nylon 6 and polypropylene phases

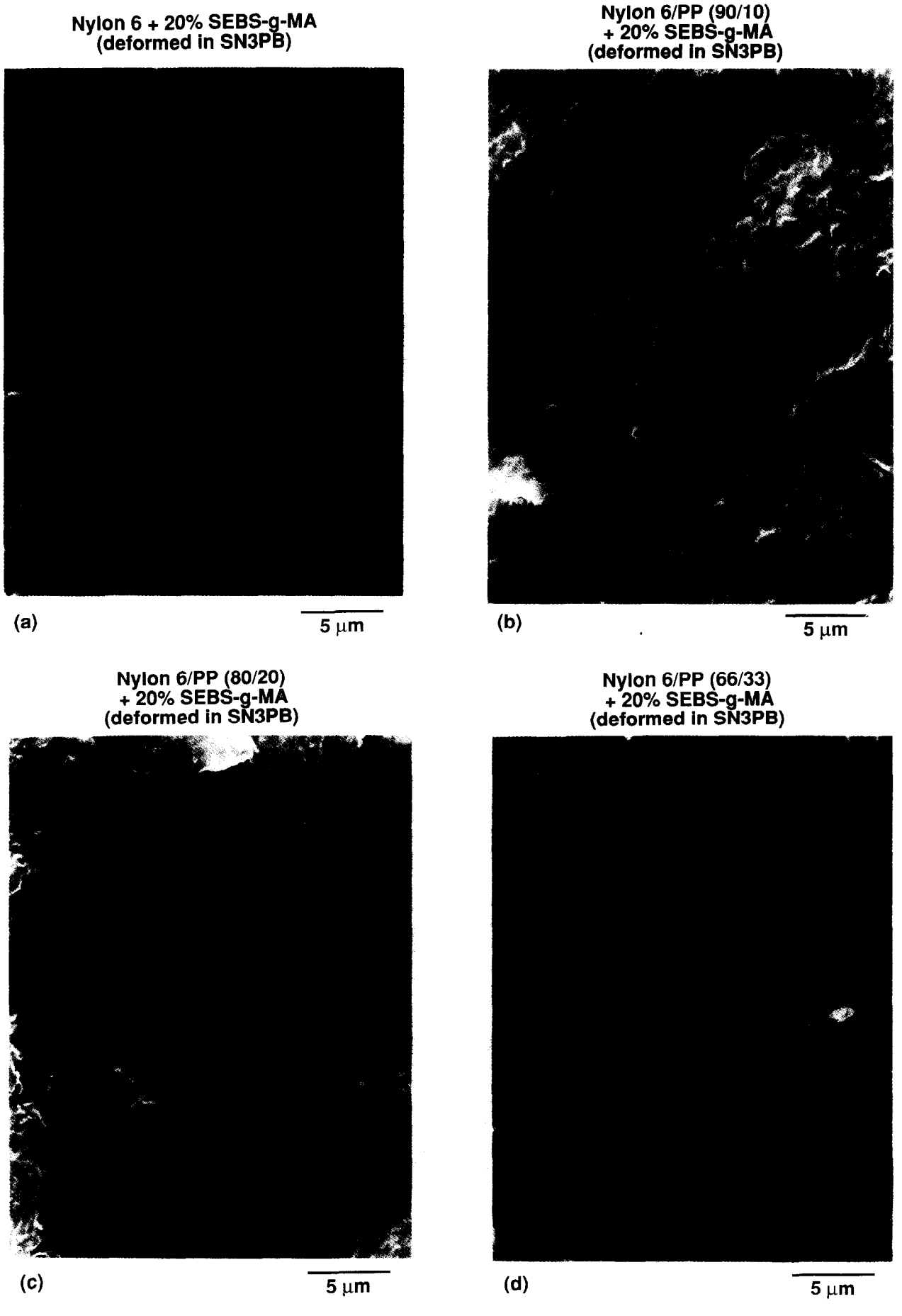

Figure 15 SEM photomicrographs of cryo-fractured surfaces of nylon 6/PP blends modified with 20% SEBS-*g*-MA and deformed in the SN3PB impact test for the following nylon 6/PP ratios (a) 100/0, (b) 90/10, (c) 80/20 and (d) 66/33

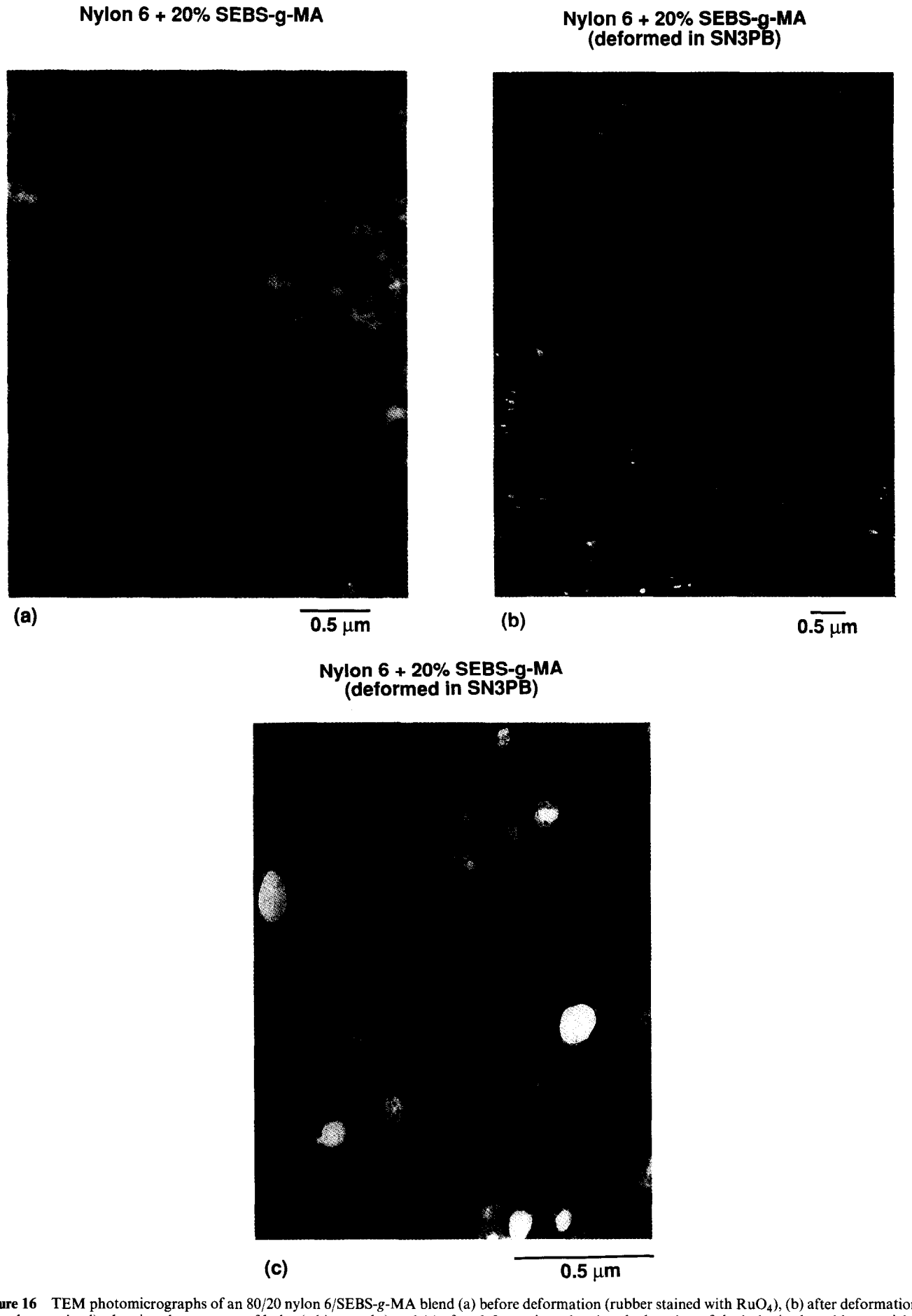

Figure 16 TEM photomicrographs of an 80/20 nylon 6/SEBS-*g*-MA blend (a) before deformation (rubber stained with RuO_4), (b) after deformation (sample unstained), showing the presence of holes (white specks) and (c) after deformation, showing the location of the holes in the rubber particles (rubber stained with RuO_4)

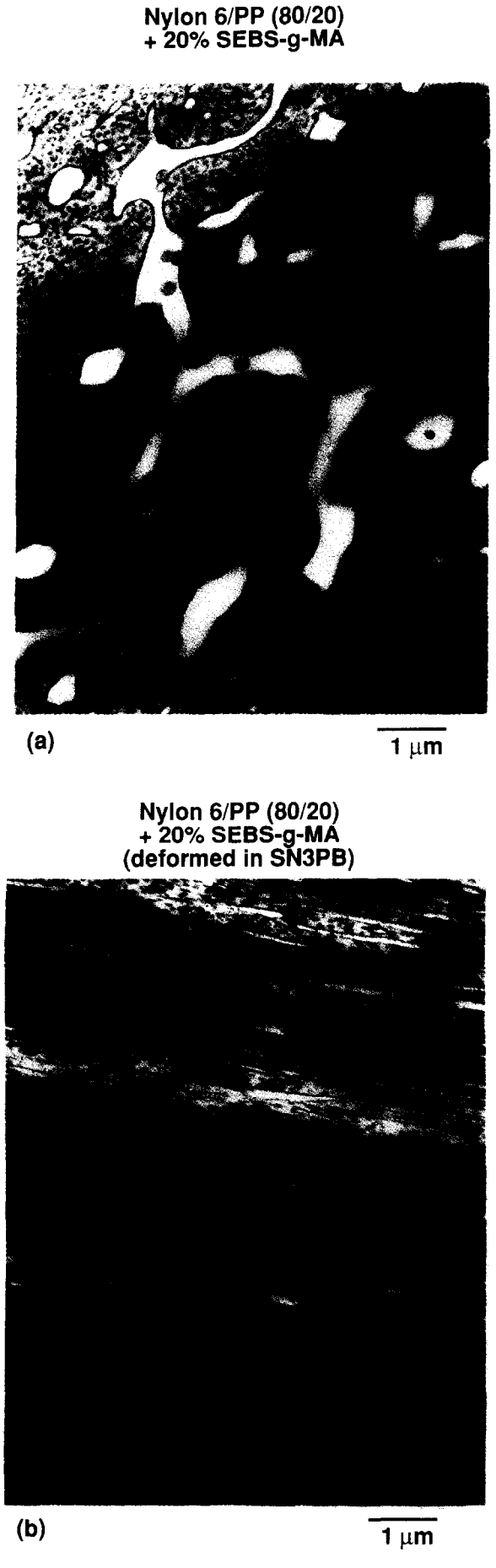

Figure 17 TEM photomicrographs of an 80/20 nylon 6/PP blend (modified with 20% SEBS-*g*-MA) (a) before deformation and (b) after the SN3PB test. The rubber is stained with RuO_4

located almost exclusively in the nylon 6 and at the interface with the polypropylene. *Figure 17b* shows the deformed sample after the SN3PB test. There is extensive deformation of the nylon 6 and polypropylene phases. The polypropylene has elongated into thin domains, while the nylon 6 phase is also highly oriented. Cavitation of the rubber particles is not detected in this photomicrograph. Thus, both the nylon 6 and the polypropylene undergo shear yielding in these blends. It appears that the stress necessary for the cavitation of SEBS-*g*-MA particles is higher than the yield stress of the polypropylene under the prevailing triaxial stress conditions ahead of the crack tip. If this is true, then the polypropylene domains yield before the SEBS-*g*-MA particles can cavitate.

CONCLUSIONS

The mechanisms of toughening in rubber-modified nylon 6/polypropylene blends were found to be a function of the type of rubber modifier, either EPR-*g*-MA or SEBS-*g*-MA, and of the ratio of nylon 6 to polypropylene in the blend.

Tensile dilatometry and electron microscopy confirm that nylon 6/PP blends modified with EPR-*g*-MA show both volume dilation and shear yielding during deformation. The extent of volume dilation varies with the polypropylene content in the blend. Dilational processes are more prevalent at the early stages of the deformation for blends where the rubber and polypropylene are dispersed in a nylon 6 matrix, whereas in blends where the polypropylene forms a co-continuous or continuous phase the dilational mechanisms become more prominent in the later stages of the deformation. Electron microscopy (SEM and TEM) revealed that the dilation results from cavitation of the rubber phase. The rubber particles dispersed in the nylon 6 phase and the rubber layer located between the nylon 6 and the polypropylene domains cavitate, giving rise to a change in volume during deformation. Similar responses were also observed in samples deformed in a high speed impact test (SN3PB).

Cavitation of the rubber particles in an 80/20 nylon 6/SEBS-*g*-MA blend was observed for specimens deformed in a high speed impact test, indicating that SEBS-*g*-MA rubber particles can cavitate under appropriate stress–strain conditions. However, nylon 6/PP blends modified with SEBS-*g*-MA showed, in general, negligible change in volume by dilatometric measurements during slow tensile deformation with the exception of the 66/33 nylon 6/PP blend, where volume dilation was detected. SEM and TEM photomicrographs showed no indication of dilational processes during the SN3PB test. The structure of the rubber modifier and its particle size are factors that contribute to the differences observed in the extent of cavitation of nylon 6/PP blends modified with SEBS-*g*-MA or EPR-*g*-MA.

ACKNOWLEDGEMENTS

This research was supported by the US Army Research Office. A fellowship for A. González-Montiel from CONACYT (Mexico's National Council for Science and Technology) is gratefully acknowledged.

REFERENCES

1 Gelles, R., Lutz, R. G. and Gergen, W. P. (Shell) *Eur. Pat. Appl. 0 261 748* 1987
2 Modic, M. J. and Pottick, L. A. *Plast. Eng.* 1991, 37
3 Modic, M. J. *Soc. Plast. Eng., ANTEC* 1993, **39**, 205
4 Modic, M. J. and Pottick, L. A. *Polym. Eng. Sci.* 1993, **33**, 819
5 Nishio, T., Yokoi, T., Nomura, T., Ueno, K., Akagawa, T., Sakai, I. and Takasaki, Y. (Toyota) *US Pat. 4 988 764* 1990
6 Hölsti-Miettinen, R. and Seppälä, J. *Polym. Eng. Sci.* 1992, **32**, 868
7 Rösch, J. and Mülhaupt, R. *Makromol. Chem., Rapid Commun.* 1993, **14**, 503
8 González-Montiel, A., Keskkula, H. and Paul, D. R. *Polymer* 1995, **36**, 4605
9 Bucknall, C. B. 'Toughened Plastics', Applied Science, London, 1977
10 Bucknall, C. B., Heather, P. S. and Lazzeri, A. *J. Mater. Sci.* 1989, **16**, 2255
11 Bucknall, C. B., Karpodinis, A. and Zhang, X. C. *J. Mater. Sci.* 1994, **29**, 3377
12 Coumans, W. J., Heikens, D. and Sjoerdsma, S. D. *Polymer* 1980, **21**, 103
13 Gaymans, R. J. and Borggreve, R. J. M. in 'Multiphase Macromolecular Systems' (Ed. B. M. Culbertson), Vol. 6, Plenum Press, New York, 1989, p. 461
14 Gaymans, R. J., Borggreve, R. J. M. and Oostenbrink, A. J. *Makromol. Chem., Macromol. Symp.* 1990, **38**, 125
15 Dekkers, M. E. J., Hobbs, S. Y. and Watkins, V. H. *J. Mater. Sci.* 1988, **23**, 1225
16 Schwarz, M. C., Keskkula, H., Barlow, J. W. and Paul, D. R. *J. Appl. Polym. Sci.* 1988, **35**, 653
17 Yee, A. F. *J. Mater. Sci.* 1977, **12**, 757
18 Yee, A. F. and Pearson, R. A. *J. Mater. Sci.* 1986, **21**, 2462
19 Sue, H.-J. and Yee, A. F. *J. Mater. Sci.* 1989, **24**, 1447
20 Sue, H.-J. and Yee, A. F. *J. Mater. Sci.* 1991, **26**, 3449
21 Sue, H.-J., Huang, J. and Yee, A. F. *Polymer* 1992, **33**, 4868
22 Ramsteiner, F. and Heckmann, W. *Polym. Commun.* 1985, **26**, 199
23 Parker, D. S., Sue, H.-J., Huang, J. and Yee, A. F. *Polymer* 1990, **31**, 2267
24 Pearson, R. A. and Yee, A. F. *J. Mater. Sci.* 1986, **21**, 2475
25 Narisawa, I. and Ishikawa, M. in 'Crazing in Polymers' (Ed. H.-H. Kausch), Vol. 2, Springer, New York, 1990
26 Lazzeri, A. and Bucknall, C. B. *J. Mater. Sci.* 1993, **28**, 6799
27 Jang, B. Z. *Polym. Eng. Sci.* 1985, **25**, 98
28 Hobbs, S. Y. and Dekkers, M. E. J. *J. Mater. Sci.* 1989, **24**, 1316
29 Maxwell, M. A. and Yee, A. F. *Polym. Eng. Sci.* 1981, **21**, 205
30 Bucknall, C. B. *Makromol. Chem, Macromol. Symp.* 1990, **38**, 1
31 Oostenbrink, A. J., Dijkstra, K., van-de-Wal, A. and Gaymans, R. J. in 'Proceedings of the Plastics and Rubber Institute Conference on Deformation and Fracture of Polymers', Cambridge, 1991, 50/1
32 Chou, C. J., Vijayan, K., Kirby, D., Hiltner, A. and Baer, E. *J. Mater. Sci.* 1988, **23**, 2521
33 Speroni, F., Castoldi, E., Fabbri, P. and Casiraghi, T. *J. Mater. Sci.* 1989, **24**, 2165
34 Flexman, E. A. *Proc. Am. Chem. Soc., Div. Polym. Mater. Sci. Eng.* 1990, **63**, 112
35 Sue, H.-J. *Polym. Eng. Sci.* 1991, **31**, 270
36 Sue, H.-J. and Yee, A. F. *J. Mater. Sci.* 1993, **28**, 2975
37 Borggreve, R. J. M. PhD Dissertation, University of Twente, The Netherlands, 1988
38 Dijkstra, K. PhD Dissertation, University of Twente, The Netherlands, 1993
39 Dijkstra, K. and Gaymans, R. J. *Polymer* 1993, **34**, 3313
40 Hobbs, S. Y., Bopp, R. C. and Watkins, V. H. *Polym. Eng. Sci.* 1983, **23**, 380
41 Keskkula, H. and Paul, D. R. in 'Nylon Plastics Handbook' (Ed. M. I. Kohan), Hanser, Munich, in press
42 Margolina, A. *Polym. Commun.* 1990, **32**, 95
43 Seo, Y., Hwang, S. S. and Kim, K. U. *Polymer* 1993, **34**, 1667
44 Borggreve, R. J. M., Gaymans, R. J. and Eichenwald, H. M. *Polymer* 1989, **30**, 78
45 Wu, S. *J. Appl. Polym. Sci.* 1988, **35**, 549
46 Wu, S. *Polymer* 1985, **26**, 1855
47 Flexman, E. A. in 'Proceedings of the International Conference on Toughened Plastics', Plastics and Rubber Institute, London, 1978, p. 14
48 Jang, B. Z. *J. Appl. Polym. Sci.* 1985, **30**, 2485
49 Jang, B. Z. *Polym. Eng. Sci.* 1985, **25**, 643
50 Ramsteiner, F., Kanig, G., Heckmann, W. and Gruber, W. *Polymer* 1983, **24**, 365
51 Bucknall, C. B. and Page, C. J. *J. Mater. Sci.* 1982, **17**, 808
52 Coumans, W. J. and Heikens, D. *Polymer* 1980, **21**, 957
53 van Hartingsveldt, E. A. A. and van Aartsen, J. J. *Polymer* 1991, **32**, 1482
54 González-Montiel, A. PhD Dissertation, The University of Texas at Austin, 1994
55 Hahn, M. T., Hertzberg, R. W. and Manson, J. A. *J. Mater. Sci.* 1986, **21**, 39
56 Flexman, E. A. *Polym. Eng. Sci.* 1979, **19**, 564
57 Borggreve, R. J. M., Gaymans, R. J. and Eichenwald, H. M. *Polymer* 1989, **30**, 78